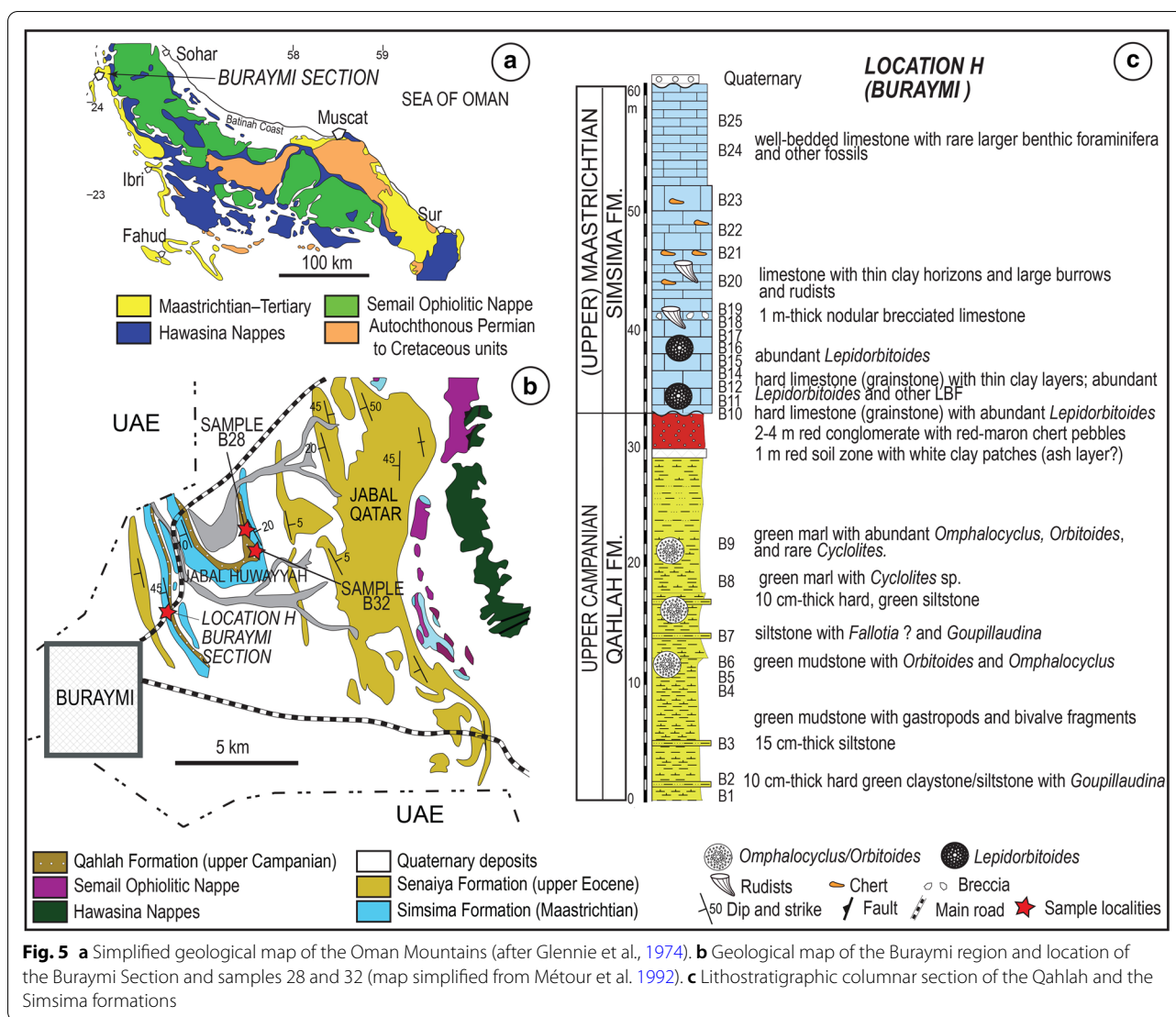


**Fig. 4** Simplified geological map of the Kahta, Adiyaman region in SE Turkey (after Özcan, 1994) and a composite lithostratigraphic log of the Terbüzek, Besni and Germav Formations with positions of the samples

immediately below the Simsima Formation (Fig. 5) (Buraymi Section in Kayğılı et al. 2021). The upper Campanian Qahlah Formation here consists of massive mudstone/marl and siltstone beds with primitive *Omphalocyclus* (*O. omanensis* sp. nov. in Kayğılı et al. 2021), *O. medius* and calcareous nannofossils with a typical late Campanian assemblage (zones CC22b and CC23a). The marine siliciclastic beds in the upper part of the Qahlah Formation are overlain by a paleosol horizon and a conglomerate bed with predominantly chert pebbles, with a sharp contact with the overlying Simsima Formation.

The Simsima Formation is of variable thickness (2.5–200 m) and is a shallow marine bioclastic limestone. Foraminifera reported from previous studies include *O. medius*, *O. apiculatus*, *O. macroporus*, *Pseudomphalocyclus blumenthali*, *L. cf. minor*, *Siderolites calcitrapoides*, *Loftusia morgani* Douvillé, *Sulcoperculina dickersoni* (Palmer) (Abdelghany, 2003; Béchenec et al.

1993; Schlüter et al. 2008; Skelton et al. 1990). Rudists are common, with assemblages including *Vaccinites*, *Hippurites*, *Durania*, *Biradiolites*, *Dictyoptychus*, *Torreites*, *Vautrinia*, *Bournonia*, *Pseudopolyconites*, and *Sabinia* (Skelton et al. 1990). In the Buraymi region, the Simsima Formation begins with a succession of nodular, resistant calcarenitic beds, 9-m-thick, with clay partings (Fig. 5). This part is highly fossiliferous, dominated by *O. gensacicus* (Leymerie, 1851), *Lepidorbitoides* ex. interc. *socialis* (Leymerie, 1851)–*minor* (Schlumberger, 1902), *Sirtina orbitoidiformis* Brönnimann and Wirtz, 1962, *Clypeorbis* cf. *mamillatus* (Schlumberger, 1902), *Ilgazina unilateralis* Erdoğan, 1995, *Siderolites* sp., *O. cf. macroporus*, *Pseudorotalia* sp., *Rotalispira* sp., *Fallotia* sp., *Planorbulina* sp., *Fissoelphidium* sp., algae, miliolids, gastropods and agglutinated foraminifera (Özcan et al. 2021). The age of the studied populations is, thus, safely constrained to the Maastrichtian, most likely to the late (not



latest) Maastrichtian by the co-occurrence of the primitive developmental stage of *L. socialis* and *O. gensacicus*, a 'late Maastrichtian' key species in Europe (Caus et al. 1996; Eggink & Baumfalk, 1983; Özcan & Özkan-Altiner, 1997). *O. gensacicus*, recorded for the first time from the Simsima Formation in Oman, is accepted as the youngest representative of the genus and thus, its presence in the Simsima Formation unequivocally suggests a late Maastrichtian age.

**Materials and methods**

Samples were collected at three localities (Localities A–C) in the southeastern part of the Central Sakarya Basin, near Nallıhan (province of Ankara), and from three localities at the Arabian Platform margin (Localities D–F) in SE Turkey (Figs. 1 and 4). Samples from

the Haymana Basin (Locality G) in Central Turkey, and Buraymi region (Locality H) in north Oman (Fig. 5), are also incorporated to this study.

*Locality A (Eğçeler A Section, Central Sakarya Basin):* 19 samples were collected to the south of Eğçeler village near Nallıhan, Ankara province (Fig. 1b). Samples 1–12 are from the massive marly beds of the Seben Formation below the sandstones of the Taraklı Formation, and samples 13–19 (sample 13: 40° 14' 6.64" N, 31° 5' 39.19" E; sample 19: 40° 14' 5.10" N, 31° 5' 39.72" E) come from the middle and upper part of sandstone succession of the Taraklı Formation. The Taraklı Formation is unconformably overlain by coarse red beds of the Kızılçay Formation.

*Locality B (Eğçeler B Section, Central Sakarya Basin):* Samples EPB 1–9 were taken from the Taraklı

Formation near Epçeler village, approximately 700 m east of Locality A, to the southeast of Epçeler village (sample 1: 40° 14' 15.01" N, 31° 5' 56.51" E; 40° 14' 6.19" N, sample 9: 40° 14' 6.19" N, 31° 6' 1.83" E).

*Locality C (Dereköy Section, Central Sakarya Basin):* Samples DE 6 and 7 were taken from the upper part of the Taraklı Formation near Dereköy village to the northwest of Nallıhan, Ankara province (sample 6: 40° 15' 51.45" N, 31° 20' 9.55" E, sample 7: 40° 15' 51.71" N, 31° 20' 9.43" E).

*Locality D (SE Turkey).* Samples TF2 and TF5 come from the middle part of the Terbüzek Formation to the west of Alıdamı, Kahta, Adıyaman province (37° 55' 38.12" N, 38° 54' 8.70" E and 37° 55' 35.54" N, 38° 54' 7.74" E) (Özcan, 1994).

*Locality E (SE Turkey).* Samples TC6-10 and 13 were collected from the Besni Formation to the north of Alıdamı, Kahta, Adıyaman province (37° 56' 6.26" N, 38° 58' 16.36" E) (Özcan, 1994).

*Locality F (SE Turkey).* Sample GA64 was taken from a turbiditic bed of the Germav Formation to the southeast of Karadut, Kahta, Adıyaman province (37° 55' 15.99" N, 38° 47' 46.44" E) (Özcan, 1994).

*Locality G (Haymana Basin, Central Turkey).* Samples DEG16-20B were collected just below the Cretaceous–Cenozoic boundary near the village of Sarıdeğirmen (39° 30' 37.21" N; 32° 26' 53.24" E) (Özcan & Özkan-Altınır, 1997).

*Locality H (Buraymi region, North Oman).* The samples B6, B8 and B9 were collected from the upper part of the Campanian Qahlah Formation near Buraymi (24° 16' 48.57" N; 55° 49' 26.96" E; 24° 16' 49.84" N; 55° 49' 24.68" E). A detailed description of the Buraymi section is given by Kaygılı et al. (2021).

The material from the Taraklı Formation consists of 359 isolated *Orbitoides* specimens studied in equatorial sections and about 50 specimens studied in axial sections, and a single *Lepidorbitoides* specimen, investigated through its equatorial section, supplemented by random thin sections. The material from the Terbüzek and Besni Formations consists of 261 *Orbitoides* specimens studied in their equatorial sections and 14 specimens studied in axial sections. Equatorial, axial and tangential sections, essential for taxonomy, require the grinding of the isolated test on preferred orientations by a fine grinding paper. The measurements and counts used in the morphometry of these taxa are shown in Tables 1 and 2. All specimens are deposited in the palaeontological collections of the Geological Engineering Department of İstanbul Technical University and prefixed EO/. For calcareous nannofossils, eleven samples from Epçeler A Section and one sample from Epçeler B Section, and five from Dereköy Section were collected.

They were prepared as simple smear slides following standard procedures (Bown & Young, 1998) and analysed through a polarised light microscope at ×1250 magnification.

### Species concept and evolutionary trends in *Orbitoides*

The definition of species in palaeontology is fraught with difficulty. On one hand, we may seek to attempt to determine that a fossil species has equivalent meaning to that of a biological species—a grouping of organisms that can interbreed and are reproductively isolated from other groups. Our recognition of species may attempt to allude to this unknowable goal. More practically, we may try to define species as distinct forms within the process of evolution, capturing the progressive stages of the evolution of a genus or related group of genera. Very often, species are defined because they seem distinct enough to a palaeontologist to merit separation. This can be very subjective, especially if the evolutionary context of the new species being described is not well understood.

The concept of species definition in larger benthic foraminifera (LBF) is a case in point. Differences in the complex internal structure of many LBF are the basis for species definition, with external morphology often a secondary consideration, as it is often viewed as being controlled by localised environmental factors. In several LBF groups, including *Orbitoides*, two approaches to species definition have arisen. The first is a *typological* approach, following long palaeontological tradition. A grouping of the size and shape of internal features, and perhaps external features, collectively define a species with reference to type specimens. This method has been described as “the intuitive appraisal of differences recognised by the specialist on the basis of his ‘experience’ ” (Drooger, 1993), in other words, the entire process of empirical pattern recognition (Less & Kovacs, 2009). The second is a *morphometric* approach, where a statistical analysis of morphological characters (such as diameter of the embryo, and size and number of peri-embryonic chambers) in an adequate number of samples from successive populations can be used to define the evolutionary stages of each character to form a bioseries. Both methods have advantages and disadvantages (Less & Kovacs, 2009; Pignatti, 1998). A potential pitfall of morphometric methods is that they consider a population of generally similar forms to be a single species, and thus, representative of the range within that species. This means that co-existing parallel lineages can be overlooked.

Since the first description of *Orbitoides* by d’Orbigny, many species have been described based on various criteria (see van Gorsel, 1978 for a historical account). Classification follows either typological (based on overall test

**Table 1** Morphometric data of *Orbitoides* from the Tarakli, Terbüzek, Besni and Germav Formations

Sample	N	Li + li		E	Mean	Species
		Range (µm)	Mean ± s.e (µm)			
EPA14	43	650.0–1310.0	919.50 ± 22.2	8–20	13.10	<i>O. ex. interc. gruenbachensis-apiculatus</i>
EPA15	38	530.0–1300.0	886.90 ± 31.2	8–17	13.00	
EPA16	25	645.0–1400.0	935.00 ± 38.5	8–18	13.33	
EPA18	9	675.0–1240.0	920.00 ± 54.5	10–16	13.56	
EPA19	13	735.0–1320.0	895.77 ± 44.5	8–17	13.40	
DE 6	24	540.0–1350.0	862.92 ± 39.7	9–18	14.30	
DE 7	37	560.0–1310.0	854.86 ± 29.5	10–19	14.00	
DEG16–20	34	665.0–1380.0	1023.4 ± 29.7	11–20	14.94	<i>O. apiculatus</i>
EPB1	7	415.0–655.0	516.43 ± 29.3	3–5	4.00	<i>O. pamiri</i>
EPB2	21	280.0–580.0	452.25 ± 20.1	3–5	3.95	
EPB3	42	325.0–600.0	422.38 ± 10.2	3–5	4.02	
EPB4	24	225.0–615.0	424.38 ± 18.4	3–6	4.04	
EPB5	17	300.0–650.0	421.18 ± 20.8	4–6	4.13	
EPB6	39	290.0–730.0	456.92 ± 17.9	4–5	4.06	
EPA14	1		330.0			
EPA16	1		385.0			
EPA17	2	330.0–600	465.0	4–4	4.0	
EPA18	10	315.0–575.0	454.5 ± 21.4	4–4	4.0	
EPA19	5	350.0–530.0	438.0 ± 31.7	4–4	4.0	
DE 7	1		475.0			
TF2	45	415.0–1155.0	700.3 ± 22.3	4–15	9.13	<i>O. megaliformis</i>
TF5	72	315.0–1050.0	698.4 ± 19.9	4–15	8.60	
B6	11	260.0–690.0	440.5 ± 34.28	4–5	4.20	<i>O. medius</i>
B8	11	260.0–600.0	450.0 ± 28.80	4–5	4.36	
B9	19	260.0–690.0	440.5 ± 34.28	4–5	4.20	
TC6	33	360.0–860.0	554.4 ± 21.8	4–9	5.23	<i>O. 'medius'</i>
TC7	27	345.0–785.0	536.5 ± 22.9	4–8	5.0	
TC8	39	360.0–950.0	525.3 ± 19.1	4–8	5.21	
TC9	6	430.0–500.0	461.7 ± 10.6	4–5	4.40	
TC10	11	395.0–780.0	523.7 ± 30.8	4–6	4.63	
TC13	28	365.0–815.0	541.1 ± 23.8	4–9	5.41	
DEG16–20	2	365.0–555.0	460.0		5.0	
B28	2	450.0–505.0	477.5 ± 19.45	4	4.0	
B32	2	510.0–545.0	527.5 ± 12.37	4–7(?)	5.5	

Morphometric data of *O. medius* (Samples B6, 8 and 9) from the upper Campanian of Oman and *O. 'medius'* from the upper Maastrichtian of Beyobası Formation (sample 16–20) are given for comparison purposes. N denotes the number of specimens. Li + li: size of the embryo, E: total number of epi-embryonic chamberlets (see Fig. 6)

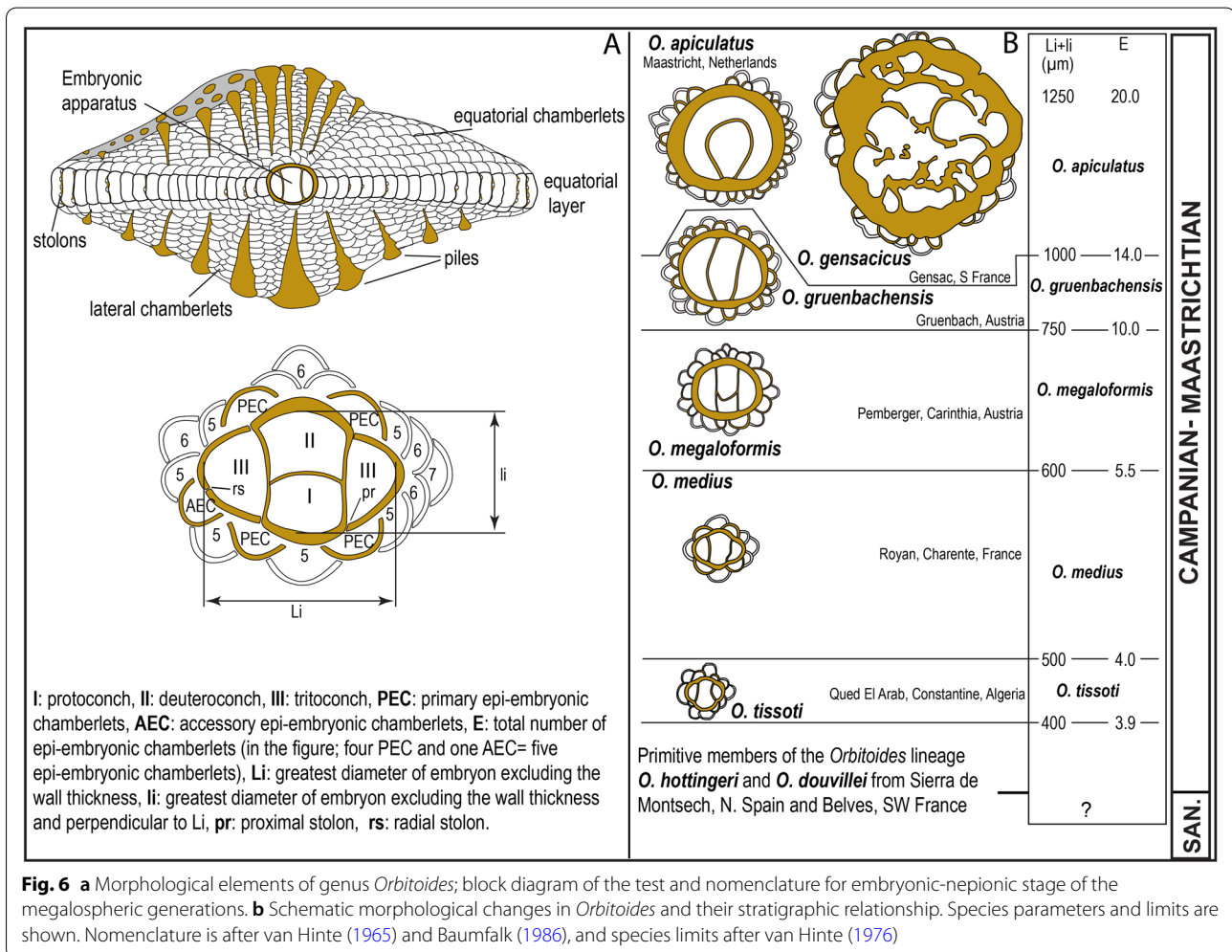
features; shape of the test, features of piles and lateral layers, type of embryonic apparatus) or morphometric species concepts. The latter approach, based on the study of the embryonic apparatus and the surrounding nepionic chamberlets, results in a single evolutionary series consisting of quantitatively defined 'chronospecies' the boundaries of which are arbitrary (Figs. 6, 7). According to this approach, all specimens from a population are assigned to a single species.

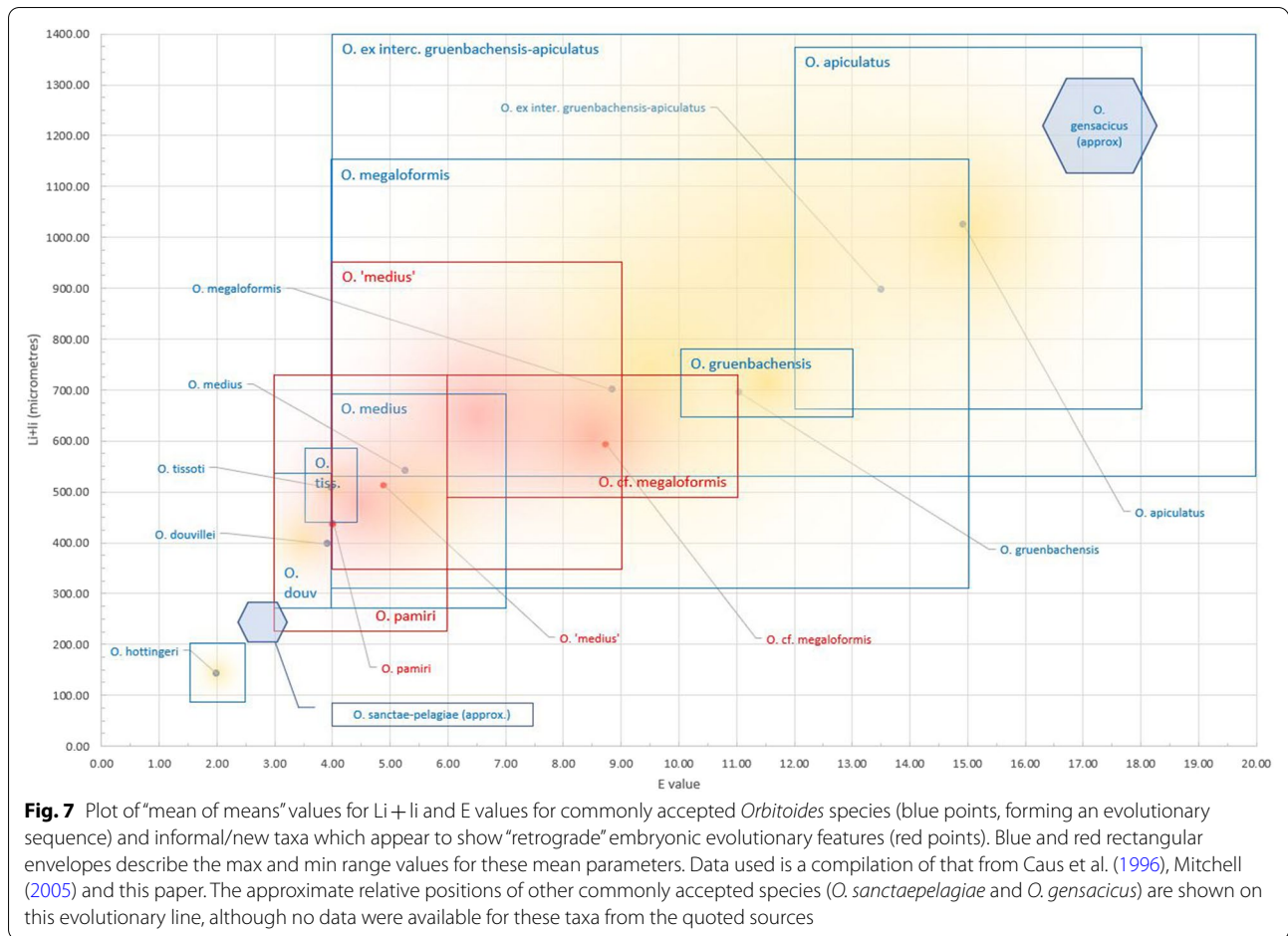
The morphological changes recorded in the equatorial layer of Late Cretaceous orbitoidal foraminifera (e.g. *Orbitoides*, *Lepidorbitoides*) are expressed by the concept of nepionic–embryonic acceleration (Drooger, 1983, 1993; van Hinte, 1966b, 1976). This is based on a progression resulting in fewer steps of chambers until the individuals attain the ontogenetic stage of cyclical development, and a tendency for an increase in the size of the embryo. In this approach to species definition, other

**Table 2** Measurements of *Orbitoides* test diameter (TD) and thickness (TT), thickness of equatorial layer in nepionic stage (EL1) and near the periphery of the test (EL2) and diameter of stolons near the periphery of test (ST)

Sa	N	TD Range and mean (mm)	TT Range and mean (mm)	EL1 Range and mean (µm)	EL2 Range and mean (µm)	ST (µm)	Species
EPA14	8	3.25–6.8 4.47	0.65–1.95 1.17	95.0–165.0 135.0	105.0–245.0 160.0	25–50	<i>O. ex. interc. Gruenbachensis– apiculatus</i>
EPA15	9	4.05–5.9 5.10	1.02–1.82 1.41	75.0–150.0 121.6	125.0–210.0 157.2	35–40	
EPA16	1	6.0	2.01	120.0	155.0		
EPA19	1	2.5	0.78	110.0	115.0		
DE 7	2	2.95–4.45 3.7	0.96	110.0–130.0 120.0	125.0–140.0 132.5		
EPB1	1	6.17	0.67	140.0	440.0		<i>O. pamiri</i>
EPB2	1	5.0	1.0	105.0	220.0		
EPB3	1	5.63	1.11	140.0	325.0		
EPB4	1	6.07	1.1	110.0	275.0		
EPB5	14	2.91–5.7 4.26	0.45–0.92 0.69	85.0–150.0 116.8	170.0–325.0 238.1	35–40	
EPB6	1	5.02	0.87	150.0	460.0		
BC6	26	1.9–5.4 3.98	0.75–2.1 1.42	85.0–140.0 113.8	130.0–205.0 157.1	25–30	<i>O. medius</i>
TC7	8	3.25–4.41 3.88	1.43–1.97 1.72	140.0–190.0 160.0	220.0–285.0 252.5	30–35	<i>O. 'medius'</i>
TC13	6	2.25–3.99 3.3	0.97–2.12 1.77	130.0–165.0 146.6	215.0–290.0 249.1	35–40	

N number of the specimens





test features, specifically shape of the test and piles, are interpreted as environmentally controlled and not used in species characterisation (van Gorsel, 1978). In contrast, Neumann (1972, 1987) concluded that primitive species of the genus (e.g. *O. dordoniensis*) actually belong to *Planorbulina* or *Planorbulinella*, and considered *O. tissoti*, *O. medius* and *O. apiculatus* as the only valid species of *Orbitoides*. Research on *Orbitoides* populations from the (upper) Campanian type section at Aubeterre (SW France) (Figs. 2, 8a), (upper) Maastrichtian type sections at ENCI quarry (St. Pietersberg, Netherland) (Figs. 2, 8b) and adjacent regions form the backbone of the morphometric studies and phylogenetic interpretations (Baumfalk, 1986; Baumfalk & Willemsen, 1986; Caus et al. 1996; Eggink & Baumfalk, 1983; van Hinte, 1966b) (Figs. 6, 7).

Key biometric features being considered as definitive include embryonic apparatus size (expressed as  $Li + li$ ) and number of epi-embryonic chamberlets (EPC) (expressed by E, total number of primary and accessory EPC). Size and number of EPC has typically been assumed to increase with time, providing biostratigraphic utility through the definition of a series of biozones (Caus

et al. 1996). Whilst this lineage is not perfectly calibrated to the standard stages of the Late Cretaceous (and bearing in mind calibration issues caused by the definition of the base Maastrichtian GSSP (Odin & Lamaurelle, 2001)), *O. gruenbachensis* Papp, *O. apiculatus*, and *O. gensacicus*, with relatively large apparatus and many epi-embryonic chamberlets (Fig. 7) are typically considered as Maastrichtian (Caus et al. 1996). It is important to note that this lineage has been defined based mostly on material from the Campanian and Maastrichtian stratotypes and allied sections in Western Europe. Can the concept of a simple single lineage be challenged by data from other Tethyan margins where *Orbitoides* proliferated (e.g. Turkey, Arabia) and from the Caribbean?

Previous studies have considered that *O. medius* and *O. megaliformis* are typical late Campanian species and the evolution from *O. medius* to *O. megaliformis* is not gradual but involves a relatively short interval of transition in which former is replaced by the latter (Baumfalk, 1986). Similarly, the evolution of *O. apiculatus* within the Maastrichtian type section involves a general increase in the embryo size and number of epi-embryonic chamberlets

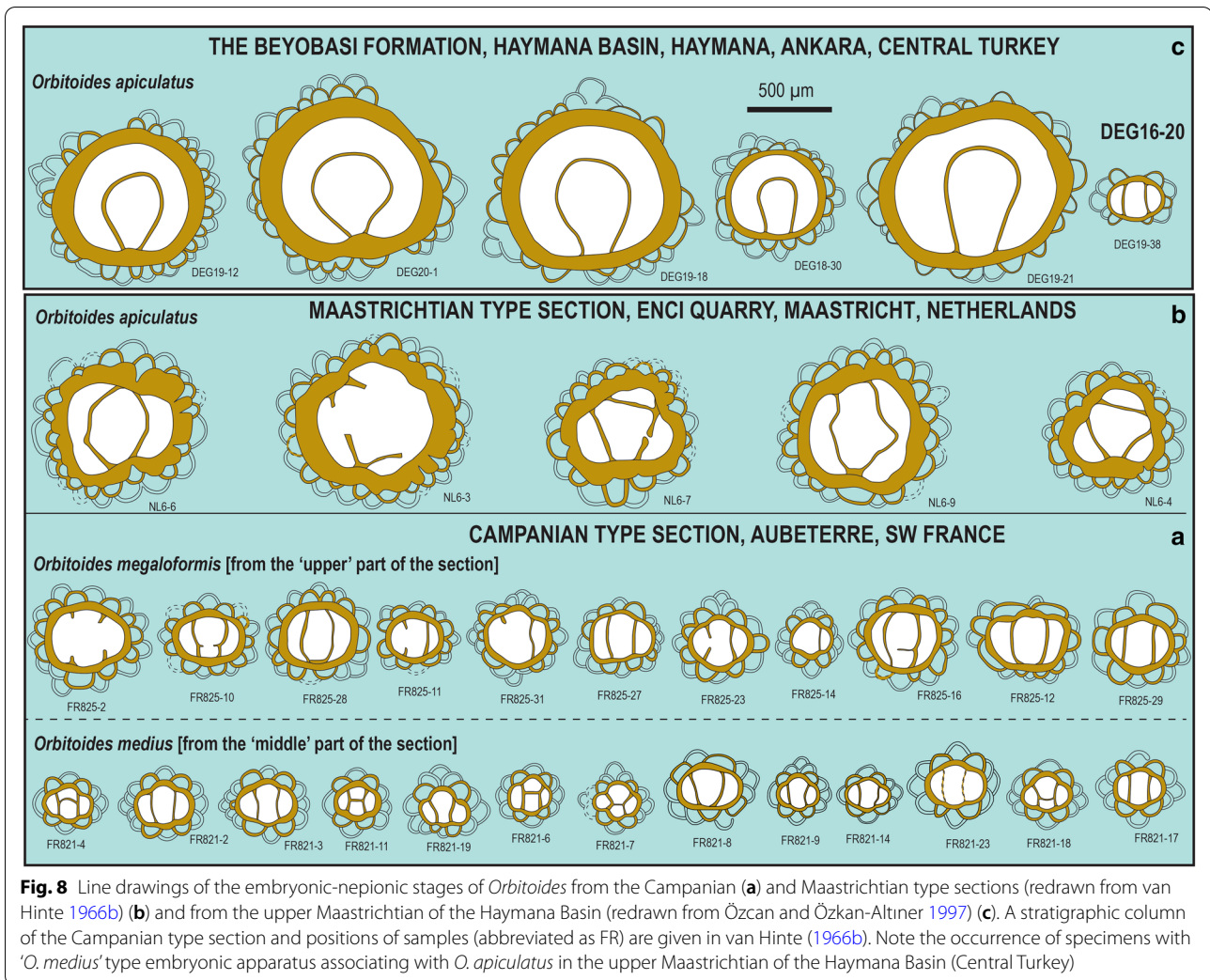


**Fig. 8** Line drawings of the embryonic-epitonic stages of *Orbitoides* from the Campanian (a) and Maastrichtian type sections (redrawn from van Hinte 1966b) (b) and from the upper Maastrichtian of the Haymana Basin (redrawn from Özcan and Özkan-Altiner 1997) (c). A stratigraphic column of the Campanian type section and positions of samples (abbreviated as FR) are given in van Hinte (1966b). Note the occurrence of specimens with 'O. medius' type embryonic apparatus associating with *O. apiculatus* in the upper Maastrichtian of the Haymana Basin (Central Turkey)

although more 'advanced' populations were recorded from the debris layers over the hardgrounds present, and the intervals between the hardgrounds contain specimens with rather smaller embryos, a phenomenon ascribed to the specific environmental conditions (Baumfalk & Willemsen, 1986).

*O. gensacicus* with a very large embryo, which is composed of a great number of embryonic chambers, was suggested to be a direct descendent of *O. apiculatus* stock in the late Maastrichtian (Eggink & Baumfalk, 1983). Thus, in spite of the uncertainties in the definition of the Campanian–Maastrichtian boundary in the shallow marine Tethyan realm, the Maastrichtian *Orbitoides* are characterised by large, tri- to quadrilocular (*O. gruenbachensis*-type), bilocular (*O. apiculatus*-type) and giant multilocular embryos (*O. gensacicus*-type).

In spite of the overall evolutionary trend in the increase of embryo size and formation of a greater number of epi-auxiliary chamberlets from the Campanian to the end

of the Maastrichtian (Fig. 7), the occurrence of *Orbitoides* specimens consisting of small embryos with only a few epi-embryonic chamberlets has been frequently reported associated with the phylogenetically advanced species such as *O. gruenbachensis*, *O. apiculatus* and *O. gensacicus* during the Maastrichtian (Baumfalk, 1986; Eggink & Baumfalk, 1983; Meriç, 1965; Özcan & Özkan-Altiner, 1997, 1999; Özer et al. 2009). These specimens were either assigned to *O. medius* as a separate species or were considered a part of the population that receives the species name based on morphometry. Meriç (1965) and Özcan (1994) thus reported *O. medius* from the Maastrichtian sequence in the Arabian Platform margin. Baumfalk (1986) has pointed out that in a purely typological sense specimens with *O. medius*-type embryos may also be found in *O. apiculatus* populations at the Maastrichtian stratotype.

The upper Maastrichtian beds, immediately below the Maastrichtian–Paleocene boundary in the Haymana

Basin (Central Turkey), yield *Orbitoides* with predominantly large bilocular embryos, but also rare small tri- to quadrilocular embryos (Özcan & Özkan-Altiner, 1997, 1999) (Figs. 2, 8c). Similarly, *O. 'medius'* was reported as co-occurring with *O. apiculatus* and *O. gensacicus* in upper Maastrichtian deposits from the Gensac–St. Marcet region in Southern France (Eggink & Baumfalk, 1983). Furthermore, Meriç (1974) reported some flat to biconcave *Orbitoides* specimens from the upper Maastrichtian of the Taurus Mountains (SW Turkey) and assigned them to *O. apiculatus pamiri* n. ssp., assuming a relationship to *O. apiculatus*. These specimens have small tri- to quadrilocular embryos and their embryonic parameters are within the limits of *O. medius* (Fig. 7). The tests of these specimens, however, are quite different from the biconvex test of *O. medius*, and the number of lateral chamberlet layers in this subspecies is much less than in *O. medius*.

## Results

### Calcareous nannofossils and age of the Taraklı Formation in the Nallihan region

Calcareous nannofossils were studied from the Taraklı Formation to provide independent biostratigraphic calibration of age. Samples from the Epçeler A and B sections contain calcareous nannofossil assemblages characterised by low abundance and poorly preserved forms (Fig. 9). However, it was possible to recognise a certain number of taxa occurring in reasonable numbers. The most abundant genus is *Micula*, mainly represented by *Micula staurophora* (Gardet) Stradner, with minor occurrences of *Micula concava* (Stradner) Verbeek and *Micula swastica* Stradner and Steinmetz (gathered under *Micula* spp.) and very rare specimens of *Micula praemurus* (Bukry) Stradner and Steinmetz. The other well-represented genus is *Watznaueria*, including *Watznaueria barnesiae* (Black) Perch-Nielsen and subordinately *Watznaueria fossacinta* (Black) Bown. Another component of the assemblages is the genus *Prediscosphaera*, well represented by *Prediscosphaera cretacea* (Arkhangelsky) Gartner and in minor amounts by *Prediscosphaera ponticula* (Bukry) Perch-Nielsen. *Lithraphidites* occurs with the presence of the marker species *Lithraphidites quadratus* Bramlette and Martini and *Lithraphidites praequadratus* Roth.

*Arkhangelskiella cymbiformis* Vekshina occurs continuously with significant numbers of medium and large specimens. Also present are *Biscutum constans* (Górka) Black and *Biscutum ellipticum* (Górka) Grün, *Retecapsa angustiforata* Black and *Retecapsa crenulata* (Bramlette and Martini) Grün. Other components are *Cribrosphaerella ehrenbergii* (Arkhangelsky) Deflandre, *Eiffellithus turriseiffelii* (Deflandre) Reinhardt, *Microrhabdulus decoratus* Deflandre, and in minor amounts *Ceratolithoides aculeus* (Stradner) Prins and Sissingh, *Chiatozygus* sp., *Cribracorona gallica* (Stradner) Perch-Nielsen, *Cyclagelosphaera* sp., *Russellia bukryi* Risatti and *Zeughrabdodus* sp. The occurrence of *L. quadratus* allows for the Epçeler Section to be attributed to the late Maastrichtian UC20a Zone of Burnett, 1998 (corresponding to the CN22 Zone of Roth, 1978 and the CC25c zones of Sissingh, 1977 and Perch-Nielsen, 1985).

Samples from Dereköy Section are characterised by low diversity calcareous nannofossil assemblages, with rare occurrences of very poorly preserved forms (Fig. 9). The main taxa are *A. cymbiformis*, *C. ehrenbergii*, *Micula* (*M. staurophora*, *M. concava* and *M. swastica*), *P. cretacea* and *Watznaueria* (*W. barnesiae* and *W. fossacinta*). Specimens occurring in minor amounts are referable to *Biscutum*, *Chiatozygus*, *Retecapsa*, and to the species *C. reinhardtii*, *E. turriseiffelii*, *M. decoratus* and *R. bukryi*. It was not possible to recognise marker species, but the occurrence of large specimens of *A. cymbiformis*, in significant amounts, and the unusual presence of the rare holococcolith *R. bukryi*, also recognised in the Epçeler Section, allows for the correlation between the two sections and the attribution of the Dereköy Section to the same late Maastrichtian age.

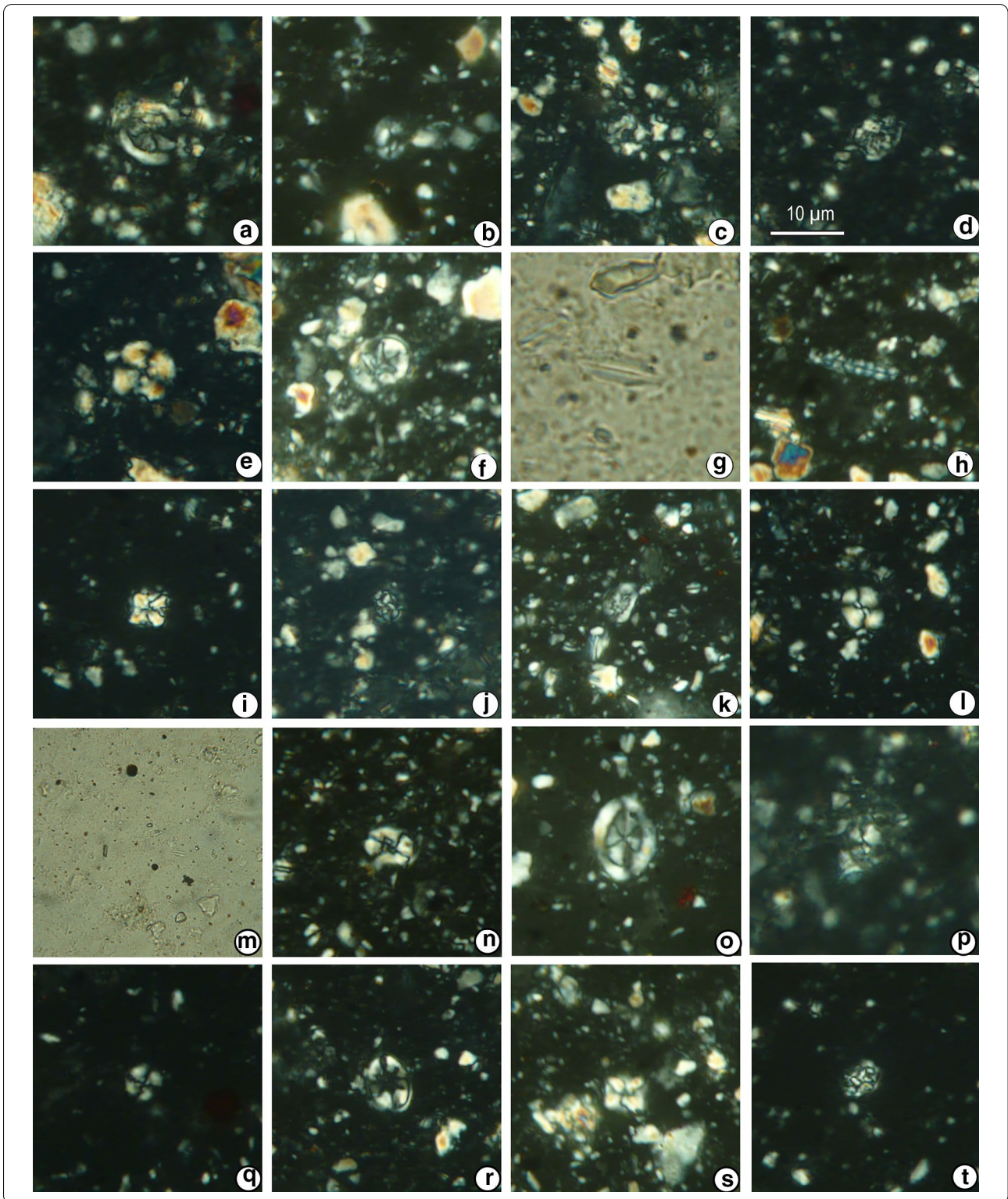
### *Orbitoides* from the Taraklı Formation

*Orbitoides* from the Taraklı Formation in Epçeler and Dereköy (localities A–C) is represented by two morphologically distinct types; lenticular, symmetrical biconvex, rarely asymmetrical tests, assigned to *O. ex. interc. grubenbachensis* Papp–*apiculatus* Schlumberger, and biconcave- to flat ones, assigned to *O. pamiri* Meriç (Fig. 10). A comparison of the test diameter versus thickness of these species, and also that of *O. 'medius'* from the Maastrichtian of Arabian Plate, is shown in Fig. 11. Although both

(See figure on next page.)

**Fig. 9** Calcareous nannofossils from the Epçeler A, B (a–n) and Dereköy (O–T) sections. **a** *Arkhangelskiella cymbiformis*, sample EPA7. **b** *Biscutum constans*, sample EPA7. **c** *Cribracorona gallica*, sample EPA7. **d** *Cribrosphaerella ehrenbergii*, sample EPA6. **e** *Cyclagelosphaera reinhardtii*, sample EPA7. **f** *Eiffellithus turriseiffelii*, sample EPA11. **g** *Lithraphidites quadratus*, sample EPA11. **h** *Microrhabdulus decoratus*, sample EPA7. **i** *Micula staurophora*, sample EPA7. **j** *Prediscosphaera cretacea*, sample EPA6. **k** *Retecapsa crenulata*, sample EPA7. **l** *Watznaueria barnesiae*, sample EPA6. **m** *Lithraphidites praequadratus*, sample EPB9. **n** *Eiffellithus gorkae*, sample EPB9. **o** *Arkhangelskiella cymbiformis*, sample DE5. **p** *Biscutum constans*, sample DE1. **q** *Cyclagelosphaera reinhardtii*, sample DE1. **r** *Eiffellithus turriseiffelii*, sample DE5. **s** *Micula staurophora*, sample DE5. **t** *Prediscosphaera cretacea*, sample DE5





species have similar test dimensions, *O. pamiri* appears to be much thinner than *O. ex. interc. gruenbachensis-apiculatus*, with a high test diameter-thickness ratio

compared to any species discussed here. A comparison of the axial sections of both species is given in Figs. 12 and 13, where the development of lateral chamberlets,



**Fig. 10** External views of *O. ex. interc. gruenbachensis-apiculatus* Papp–*apiculatus* Schlumberger and *O. pamiri* from the Taraklı Formation

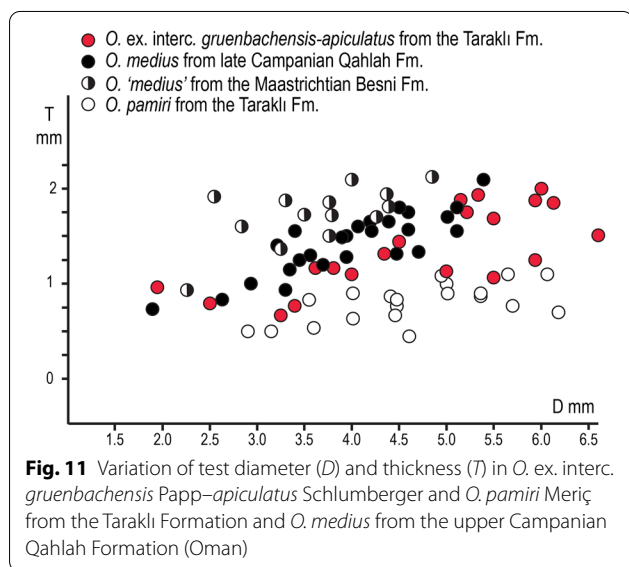


**Fig. 11** Variation of test diameter ( $D$ ) and thickness ( $T$ ) in *O. ex. interc. gruenbachensis* Papp–*apiculatus* Schlumberger and *O. pamiri* Meriç from the Taraklı Formation and *O. medius* from the upper Campanian Qahlah Formation (Oman)

thickness of the equatorial layer and stolon system are well observed. The measurements are tabulated in Table 2.

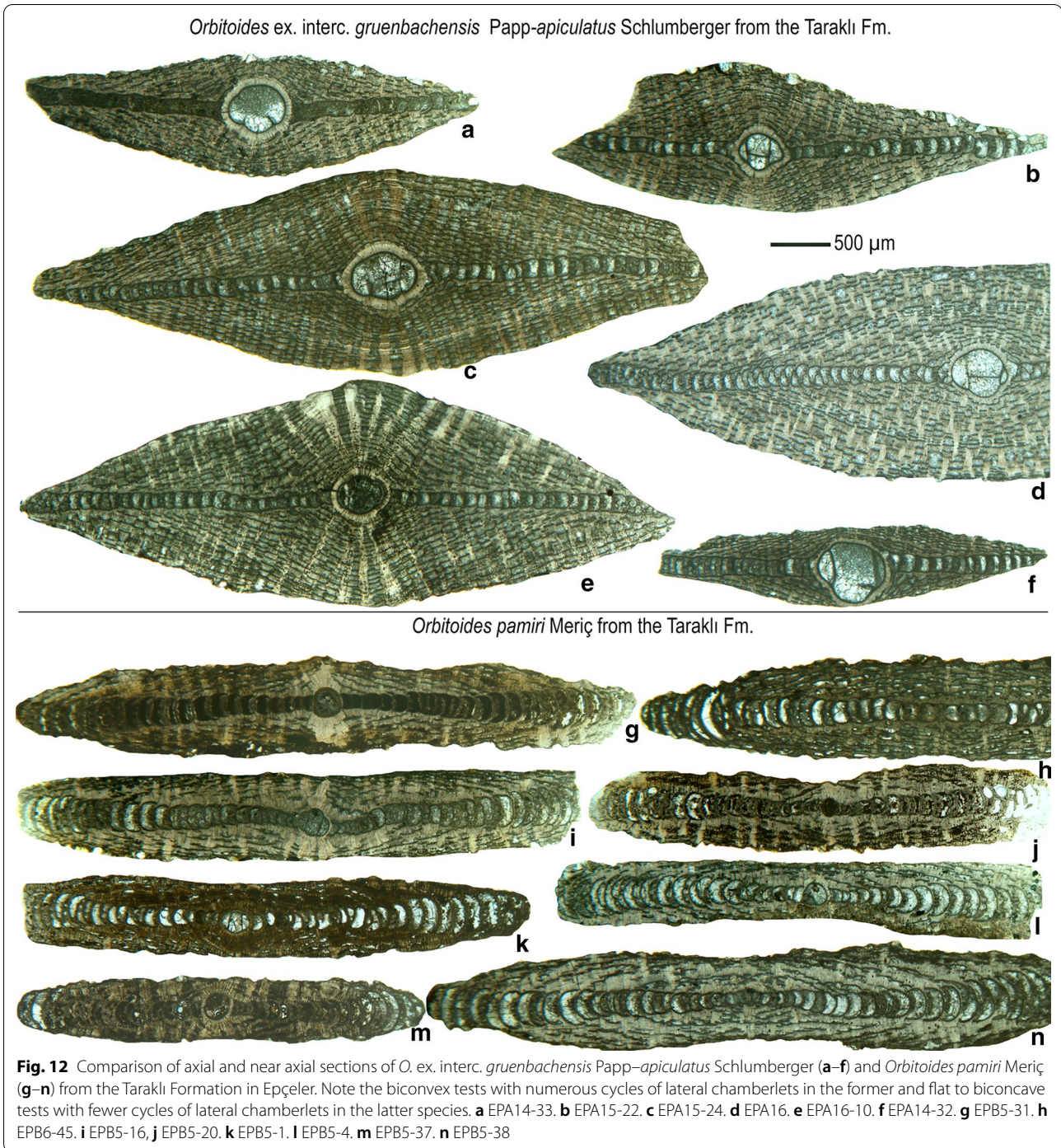
#### ***Orbitoides ex. interc. gruenbachensis* Papp–*apiculatus* Schlumberger**

In Epeçler A section, based on 21 specimens, test diameter of *O. ex. interc. gruenbachensis-apiculatus* varies between 2.95 and 6.8 mm, with sample averages ranging between 3.7 and 5.10 mm (Fig. 11; Table 2). Test thickness varies between 0.65 mm and 1.95 mm, with sample averages ranging between 0.96 and 1.41 mm. Test diameter to thickness ratio varies between 2.74 and 5.36 with

a sample average of 3.83. The thickness of the equatorial layer (excluding the chamber wall) near its centre and periphery ranges between 75 and 165  $\mu\text{m}$  and 105.0 and 245  $\mu\text{m}$  with sample averages of 132.5 and 160.0  $\mu\text{m}$ , respectively. Stolons connecting the equatorial chamberlets are about 20–25  $\mu\text{m}$  in diameter in the early stage of development and 35–40  $\mu\text{m}$  in the later stages. *Orbitoides ex. interc. gruenbachensis-apiculatus* possess predominantly large bilocular embryonic apparatus, a characteristic embryonic chamber arrangement commonly observed in *O. apiculatus* (Figs. 14a–e and 15). The average size of the embryonic apparatus ( $Li + li$ ) in seven samples from both stratigraphic sections varies between 854.8 and 935.0  $\mu\text{m}$  (Table 1). The average number of E varies between 13.0 and 14.30. These populations are assigned to a transitional development stage between *O. gruenbachensis* Papp and *O. apiculatus* Schlumberger according to the biometric species limits proposed by van Hinte (1976), which is designated as *O. ex. interc. gruenbachensis-apiculatus* (Fig. 16).

#### ***Orbitoides pamiri* Meriç**

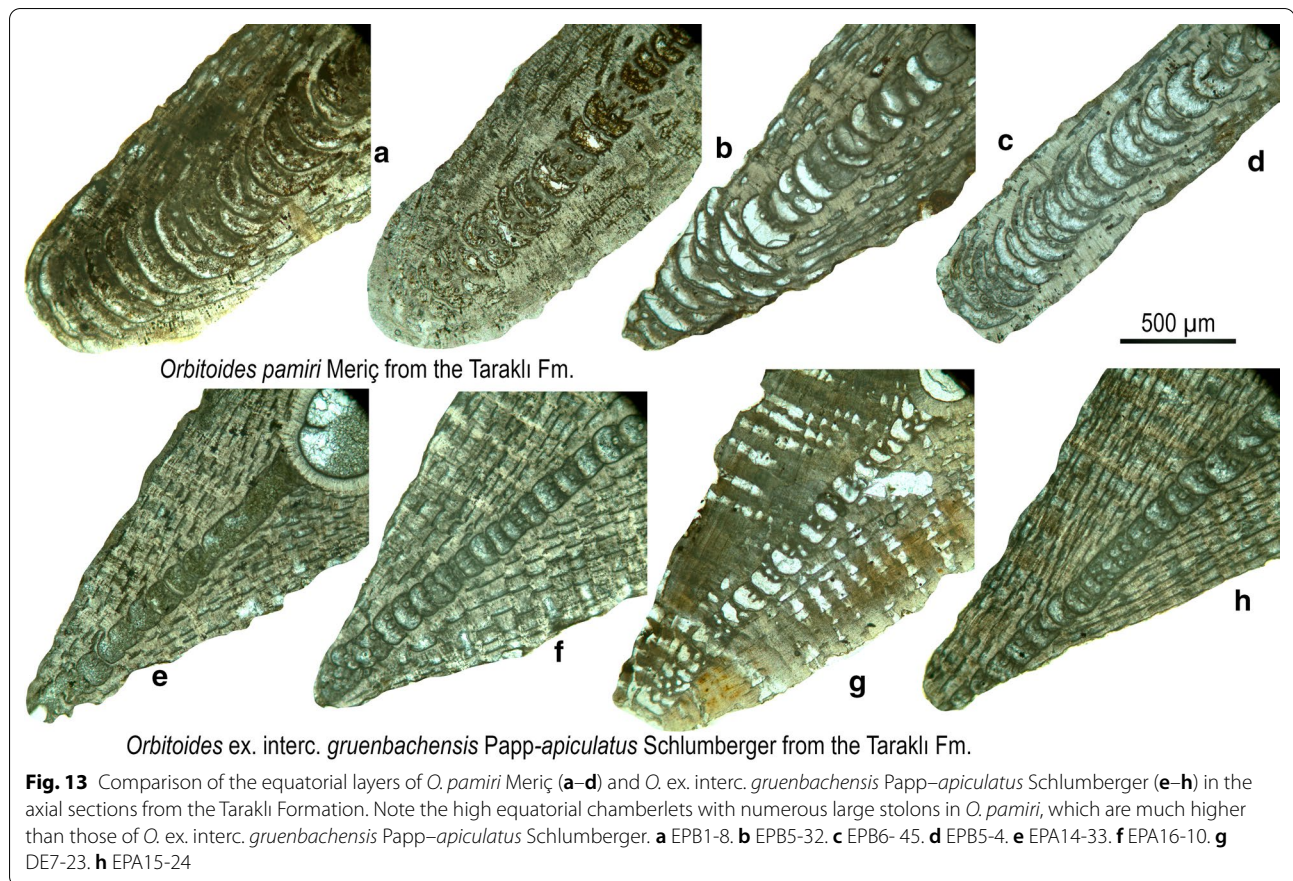
*Orbitoides* from the Epeçler B section is only represented by *O. pamiri*. Based on 19 specimens, test diameter varies between 2.9 and 6.17 mm, with an average of 4.61 mm (Fig. 11; Table 2). Test thickness varies between 0.45 mm and 0.92 mm, with an average of 0.69 mm in sample EPB5. Test diameter to thickness ratio varies between 4.33 and 10.2 with a sample average of 6.09. The thickness of the equatorial layer (excluding the chamber wall) near its centre and periphery ranges between 85 and 150  $\mu\text{m}$  and 170.0 and 440  $\mu\text{m}$ , respectively, with a sample average of 238.1  $\mu\text{m}$  in sample EPB5. Stolons connecting the



equatorial chamberlets are about 35–40 µm in diameter in the late ontogenetic stages.

*O. pamiri* from Epçeler A, B and Dereköy sections possess invariably small tri- to quadrilocular embryonic apparatus commonly observed in *O. tissoti* and *O. medius* (Figs. 14f–k, 16, 17, and 18). The average size

of the embryonic apparatus (Li+li) in nine samples from Epçeler A and B sections varies between 421.18 and 516.43 µm (Table 1). The average number of E varies between 3.95 and 4.13. It is interesting to note that some specimen of *O. pamiri* yielded embryonic apparatus with 3 epi-embryonic chamberlets (Fig. 16i and l).



### *Orbitoides* from Terbüzek, Besni and Germav Formations

*Orbitoides* specimens from the Terbüzek, Besni and Germav Formations (localities D–F) are represented by symmetrical biconvex, rarely asymmetrical tests with notably large central piles in the central part of the test. These specimens were assigned to *O. megaliformis* in Terbüzek and Germav Formations and to *O. 'medius'* in the Besni Formation.

### *Orbitoides megaliformis* Papp and Küpper

*Orbitoides* specimens from the Terbüzek Formation (Locality D; samples TF2 and 5) yielded tri- to quadrilocular embryos. The size of the embryo in both samples varies between 415.0 and 1155  $\mu\text{m}$ , and 315.0 and 1050  $\mu\text{m}$ , with sample averages of 700.3 and 698.4  $\mu\text{m}$ , respectively (Fig. 19; Table 1). The average number of epi-embryonic chamberlets are 9.13 and 8.6, respectively. This population is assigned to *O. megaliformis*, although, typologically, some specimens with small embryos and a few epi-embryonic chamberlets (e.g. TF2–18, TF2–33 in Fig. 19) are within the limits of *O. medius*. *Lepidorbitoides* from both samples invariably possess quadriserial nepionts, with a few adauxiliary chamberlets (adc) only in some several specimens (Fig. 19). In sample TF2, out

of 52 specimens, only three with one and one specimen with two adauxiliary chamberlets were found. In sample TF5, only three specimens, out of 35, with one adauxiliary chamberlets were found. These specimens with mean P, D, D/P and adc values of 98.65  $\mu\text{m}$ , 147.12  $\mu\text{m}$ , 1.5 and 0.1 in sample TF2 and 96.0  $\mu\text{m}$ , 145.71  $\mu\text{m}$ , 1.52 and 0.09 in sample TF5, respectively, were assigned to *Lepidorbitoides bisambergensis* (Jaeger) (Fig. 19).

Most *Orbitoides* specimens in the Germav Formation (Locality F; sample GA64) possess predominantly tri- to quadrilocular embryos. One single specimen yielded a bilocular embryo, typical for *O. apiculatus* (specimen GA64-84 in Fig. 19). Embryon size ranges between 410 and 910  $\mu\text{m}$ , with the sample average of 596.4  $\mu\text{m}$ . The mean E value varies between 4 and 13, with an average of 7.75. This population is assigned to *O. 'megaliformis'*, although, in a typological sense, specimen with a bilocular embryo may be assigned to *O. apiculatus*.

### *Orbitoides 'medius'* (d'Archiac)

*Orbitoides* specimens from the Besni Formation (Locality E; samples TC6, 7, 8, 9, 10 and 13) are characterised by having strongly biconvex tests with large piles in their central parts (Fig. 20). The asymmetrical tests